Tuijin Jishu/Journal of Propulsion Technology
ISSN: 1001-4055
Vol. 47 No. 01 (2026)

Enhanced Power Quality in PMBLDC Motor Drives Using Bridgeless Buck–Boost PFC Converters with Intelligent Controller

Dr. Ashok Kusagur [1], D M Srinivasa[2]

1 *Associate Professor, Department of Electrical and Electronics Engineering, University BDT College of Engineering, Davanagere 577004, India. Email: ashok.kusagur@gmail.com*

2 *Associate Professor, Department of Electrical and Electronics Engineering, P E S College of Engineering, Mandya, India.Email: dmsrinivasa.pesce@gmail.com*

Abstract: This study presents a comparative analysis of various controllers employed in power factor correction (PFC) converters used for Permanent Magnet Brushless DC (PMBLDC) motor drives. A Bridgeless Buck–Boost converter-based BLDC drive is extensively examined with respect to power factor correction capability and Total Harmonic Distortion (THD), using both Proportional–Integral (PI) and Adaptive Neuro-Fuzzy Inference System (ANFIS) controllers. The outcomes of this investigation serve as a guide for selecting the most suitable converter topology for PMBLDC drives, based on performance indices such as input power factor, harmonic distortion, power density, system size, and cost. Simulation studies are conducted to illustrate the performance differences among the controllers in terms of power quality parameters, particularly input power factor and THD. In addition, this work outlines a simplified closed-loop speed-control strategy for PMBLDC motors. The speed regulation characteristics of the PFC-fed PMBLDC drive are evaluated under varying load torques using PI and ANFIS controllers. MATLAB/Simulink is employed to provide a reliable and flexible platform for modelling, analysis, and performance validation. The proposed control method effectively suppresses torque oscillations and demonstrates high accuracy and robustness. A bridgeless PFC buck–boost rectifier is proposed to mitigate harmonic currents in the BLDC motor drive and to enhance the overall input power factor. In comparison with conventional bridged PFC rectifiers, the bridgeless topology significantly reduces conduction losses associated with the input diode bridge of the typical Voltage Source Inverter (VSI)-fed BLDC motor drive. The use of a bridgeless boost configuration consequently leads to improved conversion efficiency. Simulation results further confirm the improvement in input power factor and reduction in harmonic content achieved by the bridgeless PFC buck–boost converter. This work presents the digital simulation and performance evaluation of a PFC buck–boost converter supplying a VSI-fed PMBLDC motor drive, in which the VSI functions as an electronic commutator. The findings highlight the effectiveness and practicality of using bridgeless PFC topologies and advanced control strategies such as ANFIS for enhancing the dynamic and steady-state performance of PMBLDC drive systems.

Keywords*:* Power Factor Correction (PFC), Permanent Magnet Brushless DC Motor (PMBDCM), Total Harmonic Distortion (THD).

INTRODUCTION

The three-phase armature and the permanent magnet rotor makes the Permanent Magnet Brushless DC motor (PMBLDCM) which looks like a variant of the induction motor. The smooth operation of the motor due to the electronic commutation of PMBLDC motors makes it advantageous than induction motor in applications where constant speed is needed. The mechanical commutator which increases the wear and tear on the motor due to the friction is avoided due to the electronic commutation. Three rotor position sensing hall sensors finalize the

commutation. The permanent magnet of the motor rotates and the armature of three phase windings remain static. Adjustable speed drives (ASD) have become a possibility considering the rapid development in the power switches and the microelectronics. Both PMBLDC and the Permanent Magnet Synchronous Motor (PMSM) is widely used for ASD while exhibiting trapezoidal back EMF and sinusoidal back EMF respectively. Better controllability, better power density, high torque inertia ratio and efficiency are few important advantages that make both the motors applied on the ASD. Between these motors PMBLDCM which possess simple controllability, high efficiency and torque costing less on maintenance is applied on different industrial applications including automotive, medical, industrial automation and aerospace domain. Unlike the other motors the PMBLDCM inculcates best performance characteristics including its reduced inertia, high speed response to excitation, the power density improvement, reliability improvement, better speed control characteristics, less maintenance and high efficiency. The cooling mechanism of the motor is each as the rotor generates very less heat. The higher torque output generated by the PMBLDCM with lesser size increases the power density are the few characteristics which attracts different applications to use the PMBLDCM. The only difference in the operation between the PMBLDCM and the conventional commutated DC permanent magnet motor is that there is no commutator action in the PMBLDCM and also the brushes action. The absence of the brush and the commutators automatically eliminate the radio frequency interference that is evident while brushes are available which leads to sparking thus making PMBLDCM to be able to work for a long time continuously. Due to this advantage the PMBLDCM is utilized in the applications like the electrical vehicles and applications where the motor has to run for a longer time and where the higher heat generation due to continuous operation is a possibility. Several soft switching based PMBLDCM drives is developed which combines the advantages of speed control when the conventional PWM is utilized while also considering the capability of the resonant converters to obtain the soft switching during the period of last two decades. The low starting current and the soft switching of the converter is an advantage of the drive using PMBLDCM with resonant converter. Any motor control technique would utilize the torque ripple minimization and starting current reduction as its major criteria along with the speed control. Any nonlinear control algorithm will work without delay and more dynamically if intelligent systems are implemented.

The performance evaluation and improvement for the nonlinear mapping of the input to the dynamic torque production mechanism in the PMBLDCM is a challenging task. Thus, the learning algorithms with expert system is a solution for this nonlinear mapping. The intrinsic ability of the expert systems like the fuzzy logic and the Artificial neural Network to model the non-linearity with thin itself the uncertain and nonlinear parameter variation can be modeled with the expert systems with high robustness. The theoretical background of the traditional control methods will also help in better modeling the system with better steady state and transient characteristic's knowledge. Thus, a hybrid system would have a better modeling of the system.

Modeling

The complete control of the PMBLDCM depends on the amount of armature current supplied to it by means of varying the PWM control to the inverter by getting the position using the decoders. The electronic commutation action of the PMBLDCM makes the motor more advantageous both due to the frictionless working as brushes are absent and the robust control due to the PWM control. Rational behavior of the motor is developed using the modeling of the machine and the control algorithm which facilitates the testing of the motor in different working conditions. Unlike the hardware redesigning which is a highly expensive operation to test the motors the simulation using the modeling would be of importance especially because it can be tested for the robust operation in the dynamic conditions. Modeling and the simulation of the machine's control algorithm is a cost saving entity that would be of prime importance while carrying out the research on the domain.

An accurate model of the PMBLDCM is designed comprising the actual back EMF waveform in the model developed by Jeon et al (2000). The back EMF waveform obtained would show deviation in the actual PMBLDCM unlike that which is observed in the ideal waveform. The back EMF waveform obtained from the PMBLDCM thus modeled gave near in situ waveforms thus is providing the chance for accurate analysis [1].

Though the transfer function model is a better way of analyzing the dynamic operation of the machine the transfer function model is not completely advantageous in several terms. A transfer function-based model of the BLDC motor is developed by Navidi et al (2009). The modeling of the PMBLDCM using PSIM and Matlab GUI is developed by Rakesh Saxena et al (2010) and Balogh Tiber et al (2011) respectively [2-3]

PWM Techniques

The comparison of the bearing currents in the PMBLDCM while there is a soft and the hard switched voltage source inverter (VSI) used by emulating the same by excitation of the motor bearing using both the sine and the square wave is discussed by Subhashish Bhattacharya et al (1999) [4].

The sensor less control of high speed PMBLDCM is considered and a comparison between a Variable DC link voltages-based inverter with the ordinary PWM inverter is discussed by Kyeong Hwa Kim et al (2002) [5].

The issue of commutation delay that occurs during the high-speed operation is attended by implementing the sensor less operation of the variable DC link-based inverter. The inactive phase in the BLDC motor would create the diode freewheeling effect which is eliminated by using a novel PWM method as discussed by Wei Kun et al (2004) [6].

The novel PWM method would continue the 30-degree mode of conduction in the last switching mode to 60-degree mode in order to avoid the freewheeling mode in the diode. A four-switch inverter-based drive is used to drive the three phase BLDC motor for a reduced switches implementation and it is observed that the dynamic response obtained is satisfactory with reduced conduction losses in the literature by Dhawale et al (2010) [7].

A two-state variable technique is used to develop a very simple digital PWM method to regulate the speed in the PMBLDCM which is developed by Alphonsa Roslin Paul (2011) [8].

A PI controller-based Matlab simulation of a nonlinear model is developed and with four switch converters for the PMBLDCM control by Krishna Kumar and Jeevanandham (2011). A current controller technique is designed for a better static speed torque characteristic [9].

Voltage Source Inverter based control:

A unipolar PWM method-based torque ripple reduction algorithm is developed by Tae Sung Kim et al (2001) on a traditional BLDC drive. Along with the current dynamics the harmonics is found to be reduced by the use of the PWM technique. The harmonic component is used to generate the Space Vector Pulse Width Modulation (SVPWM) by converting to the stationary reference frame. The reduction and noise and current ripple are observed [10].

Decaying phase back EMF method is utilized for torque ripple reduction by Byoung Hee Kang et al (2001) analysis is carried out on the torque ripple obtained in the commutation period [11].

The torque ripple developed during the commutation between the incoming and the outgoing switching sequence is compensated in the control technique developed by Sang Hyun park et al (2003) [12].

Even the number switches used in the novel technique is four switches which reduces the switching loss as well. Direct Torque Control (DTC) based torque ripple reduction method is used to get the dynamic torque response as developed by Yong Liu et al (2005) [13].

A Laplace Transform based circuit analysis where the input dc voltage is varied for the speed control of the PMBLDCM is developed with the advantage of torque ripple reduction in the drive system. The technique is developed by Ki Yong Nam et al (2006) which is giving 10% decrease in the torque ripple [14].

A combination of two phase and the three phase switching mode is introduced in the novel commutation interval torque ripple reduced speed control technique in a DTC controlled PMBLDCM drive system developed by Liu et al (2006). The commutation ripple is reduced by switching from the conventional two phase switching to the

three-phase switching at the period of current commutation interval. The observed results are proved to be reducing the torque ripple successfully [15].

The design variation like pole shifting combined with the process of shaping the rotor pole is introduced in the Interior PMBLDCM (IPMBLDCM) for the torque ripple reduction in the commutation interval by Parag Upadhyay &Rajagopal (2006). The mutual torque is reduced by proper excitation while the cogging torque is reduced due to the pole shaping and the shifting of pole as claimed by the authors [16].

A torque ripple reduction method using the back EMF and currents in the three-phase input to the PMBLDCM on a DTC drive by Jianfei yang et al (2009), unlike the traditional method where flux linkage observation is required. Though the back EMF is not trapezoidal unlike the ideal waveform the reduction of torque reduction is carried out by the use of the technique [17].

A detailed torque ripple reduction technique is discussed by Somesh Vinayak Tewari & Indu rani (2009) while a non-ideal trapezoidal back EMF waveform is occurring in the PMBLDCM [18].

The torque ripple comparison with four different PWM techniques are analyzed in a comparative analysis carried out by Chuang et al (2009), by observing the phase currents that occurs during the commutation interval [19].

A two-phase conduction scheme with four switch inverters on a DTC controlled PMBLDCM drive is applied by introducing a novel lookup table method. A look up table with the back EMF versus the position of electrical rotor is considered for the speed control of the PMBLDCM by Salih Baris Ozturk et al (2010). The torque ripple during low frequency operation and the dynamic response of torque is found to be improved as compared to conventional four switch PWM current and voltage-controlled BLDC motor drives [20].

A DTC controlled PMBLDCM drive system developed by Salih Baris Ozturk & Hamid Toliyat (2011) uses the sensor less control using the simple control method. Similar to the conventional DTC scheme both the torque and the flux are controlled separately and simultaneously reduces the commutation torque ripple [21].

A novel technique of adding an extra source at the non-commutating phase in the commutation interval is discussed by Sangsefidi et al (2011). A capacitor that is charged while there is non-commutation period is discharged during the commutation period to eliminate the torque ripple during the commutation period. It is claimed by the author that there is a reduction of about 48% torque ripple[22].

The traditional speed control implementation is having a constrained speed regulation which allows the speed to be controlled to a very little variation from the rated speed. One among the advanced speed control scheme which controls the speed in a wide range is introduced by Kai Sheng Kan and Ying YU Tzou (2011). The control algorithm is an adaptive wide-angle technique producing the modulation pulses which gets adjusted for different reference speed range optimizing the efficiency. For a particular reference speed and a given load the amount of current drawn from the drive system is lower than that of the current drawn due to 120-degree mode of conduction including the reduction in torque ripple [23].

PFC Based Control of PMBLDC

A bridgeless AC-DC converter is proposed from the literature [66] that is utilized for the BLDC drive simulation. The proposed buck-boost converter with the bridgeless topology is introduced for the VSI fed BLDC drive system as shown in figure 4.1.A discontinuous inductor current is an important property of the converter that helps in achieving the PFC at the AC side of the converter. The armature voltage control-based BLDC motor speed control is achieved. The DC link voltage is controlled to attain the desired speed. The usual control technique that utilizes the VSI switching control would introduce the higher switching losses. The switching control of the VSI is at the fundamental frequency switching. The fundamental frequency operation of the VSI reduces the losses of switching. The speed control technique is validated for the higher range of speed and good power quality at the AC side. It is evident from the Figure 4.1 that the PMBLDC motor is controlled from the buck boost converter only not by the different PWM from the VSI. The speed difference to the DC-DC

converter PWM generation is a separate loop which creates the PWM from the difference in the speed signal and another loop which just checks the position of the PMBLDC motor for rotation in that particular speed.

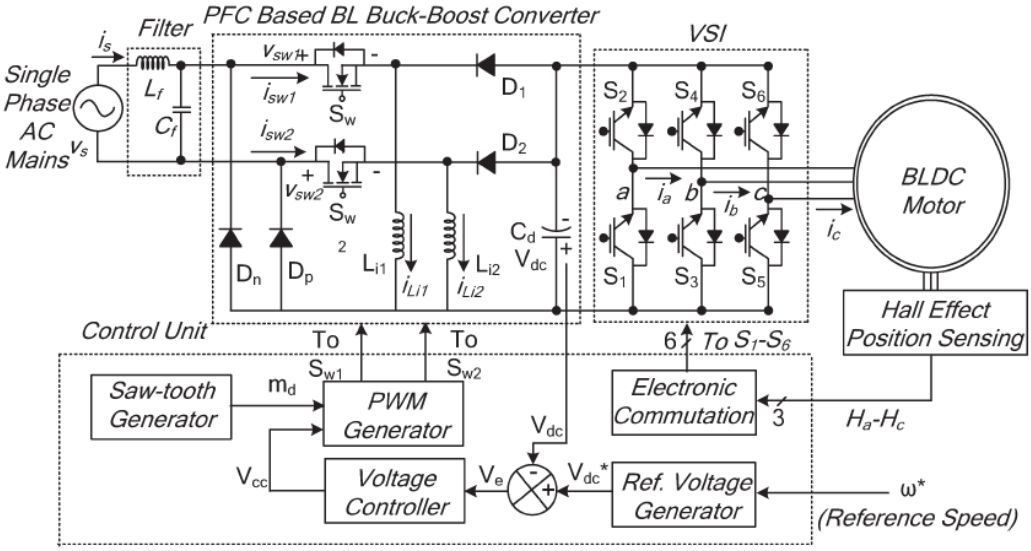

Figure 4.1 Overall Block Diagram of the Buck Boost converter-controlled BLDC drive

The topology considered for the current implementation that is considered in Figure 4.1 is defined in [66] and the operating principle of the control of the proposed controller is defined as below.

4.3 OPERATING PRINCIPLE OF PFC BL BUCK–BOOST CONVERTER

Both the positive and the negative half cycle operation is evaluated to know the operation of the proposed converter. The operation of both the cycles are as discussed below. The switching sequence of the switches Sw1 and Sw2 during its operation in both the half cycle is as discussed. The power transfer from the AC source to the DC link Cd of the converter takes its path through switch Sw1 while switched ON, inductor Li1, and diodes D1 and the positive half cycle diode as shown in Fig.4. 2(a)–(c). Similarly, the negative half cycle is conducting as shown in Fig.4. 3(a)–(c).

There is a discontinuity of the inductor current in both the half cycles in order to attain the soft switching attained in the switches for reduced switching losses. The source voltage and current through both the inductors are as shown in Fig. 4.2(d) on both the half cycles.

4.3.1 Operation during complete switching cycle

The positive half cycle of the input side AC signal would provide multiple mode of operation in the converter. Those modes are as given below,

Mode, I starts with the short circuit of the inductor Li1 across the supply through switch Sw1 and the diode Dp as is shown in Figure 2(a). The current in the inductor increases. While at the same time the capacitor at the DC link discharges the power it has accumulated in the previous modes, to the BLDC drive system.

During Mode II the switch Sw1 switches off and thus the short circuit across the inductor is lost. Then the inductor is connected directly to the dc link capacitor through D1, thus discharging the complete charge to the capacitor depicted in Figure 2(b). The inductor will drain the current and reach zero current

The discontinuous conduction mode of the inductor can be realized in Mode III as there is zero current in it. Thus there is no switch or the diode conducting in this mode as the inductor current would continue to be at zero after this as shown in Figure 2(c). The capacitor Cd continue to supply the drive side. The voltage across that

capacitor would tend to decrease. Thus by sensing that the voltage has come down the PWM controller would switch the Sw1 switch to continue the same operation further.

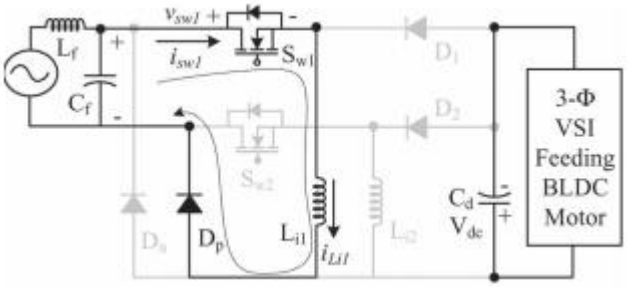

(a)

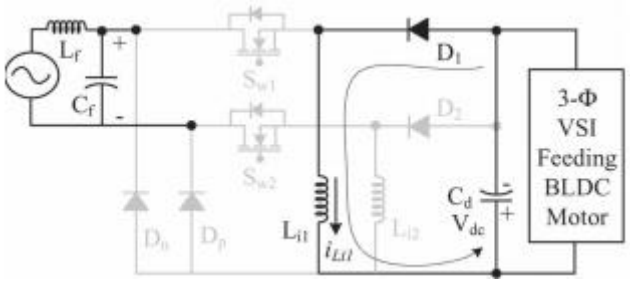

(b)

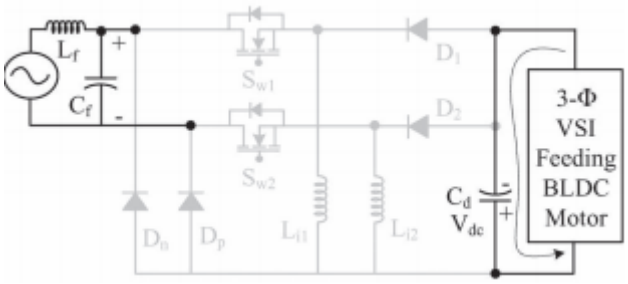

(c)

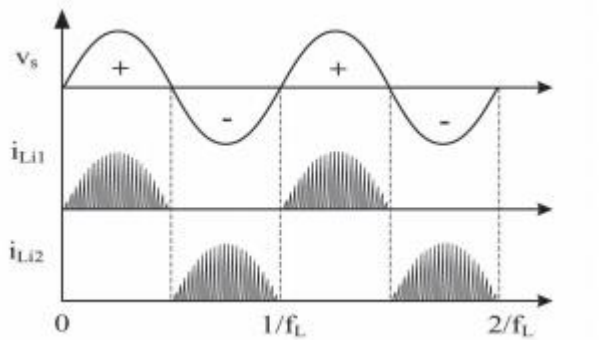

(d)

Fig. 4.2. BL Buck boos converter MODES MODE I in (a) ,MODE II in (b) and MODE III in (c). Inductor current waveform in (d) for both the half cycles.

The same operation is carried out with the set of Sw2 switch with inductor Li2. And the freewheeling using the diode D2 through the Li2 and the capacitor Cd.

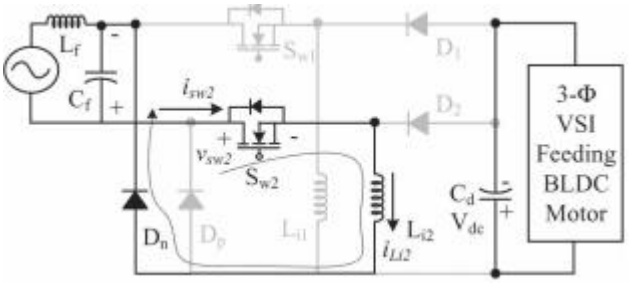

(a)

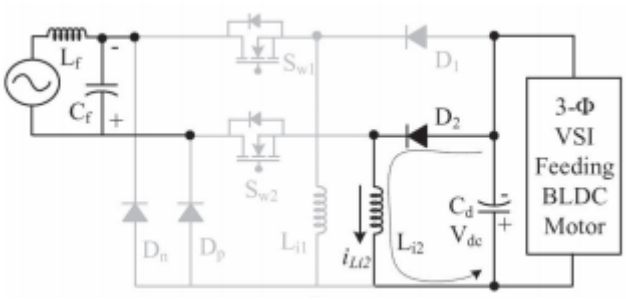

(b)

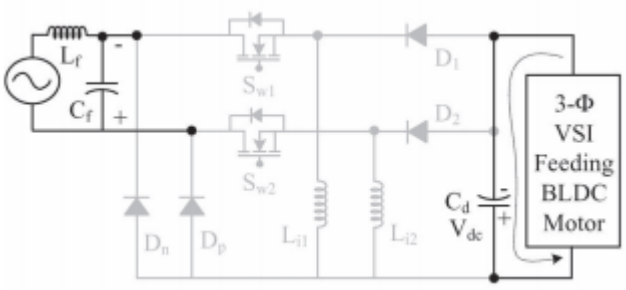

(c)

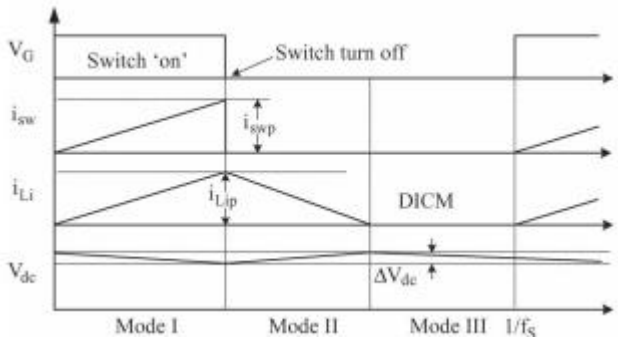

(d)

Fig. 4.3. MODE I (a), MODE II (b), MODE III (c) in negative half cycle of the proposed converter, (d) gate pulse, switch current, inductor current and output voltage

4.5 Design details of BL BUCK-boost converter

A 5HP motor with 100V operation is made to be controlled by the BL buck boost converter and inverter pair. The converter is made to operate at discontinuous conduction mode during the switching period itself thus

making a space for the soft switching of the switches. The average output voltage that is obtained if the rms value of Vs is supplied is ,

$$V_{\text{in}} = \frac{2\sqrt{2}V_s}{\pi} \quad \text{……..(4.1)}$$

Duty cycle of the buck boost converter is as given below,

$$d = \frac{V_{\text{dc}}}{V_{\text{dc}} + V_{\text{in}}}. \quad (4.2)$$

A. The Li1 and Li2 inductor design

Inductor Li1 design is defined as in equation (4.3) where is the critical conduction mode duty cycle ,equivalent load resistance is R fs is the switching frequency.

$$L_{\text{ic1}} = \frac{R(1-d)^2}{2f_s} \quad (4.3)$$

The minimum value of the inductance Li1(Lic1) is at the duty cycle where it just reaches the discontinuous conduction mode. It is called dmin. From (4.4), the calculation of Licmin is done at the duty cycle dmin.

$$L_{\text{ic min}} = \frac{V_{\text{dc min}}^2}{P_{\text{min}}} \frac{(1-d_{\text{min}})^2}{2f_s} \quad (4.4)$$

Thus to get the complete discontinuous operation the value of the inductor is considered to be as less as 1/10 th of the minimum inductance value defined in (4.4).

4.3.1 DESGN OF DC link Capacitor

Determination of the second order harmonics is prime in order to find the dc link capacitor design . The derivation of the capacitor design needs the calculation of the power input Pin in the state. The precondition that the voltage and the current at the AC source side to be in phase is important thus the equation 4.5 defines the power input from the AC side as

$$P_{\text{in}} = \sqrt{2}V_S \text{Sin}\omega t * \sqrt{2}I_S \text{Sin}\omega t = V_S I_S(1 - \text{Cos}2\omega t) \quad 4.5$$

There are two terms in the power , first term being the fundamental term and the second term being the second order term. DC link capacitor current involving in the

$$i_C(t) = -\frac{V_S I_S}{V_{\text{dc}}} \text{Cos}2\omega t. \quad (4.6)$$

To find the capacitor value the ripple value for the output voltage has to be assumed and the following equation is used to find the capacitor value,

$$\Delta V_{\text{dc}} = \frac{1}{C_d} \int i_C(t)dt = -\frac{I_d}{2\omega C_d} \text{Sin}2\omega t. \quad (4.7)$$

Considering 1% ripple value the capacitor value is rewritten as in equation (4.8).

$$C_d = \frac{I_d}{2\omega\Delta V_{\mathrm{dc}}}. \quad (4.8)$$

$$C_d = \frac{I_d}{2\omega\Delta V_{\mathrm{dc}}} = \frac{P_o/V_{\mathrm{dc\,des}}}{2\omega\Delta V_{\mathrm{dc}}} \quad (4.9)$$

After finding the capacitor value the ripple is considered as 3% and proceeded.

Source Side filter Lf and Cf design

The harmonics should not be reflected in the supply current and thus it must be absorbed using the capacitor and inductor combination of the filter. The capacitor's maximum value is as given in the equation 4.10.

$$C_{\max} = \frac{I_{\mathrm{peak}}}{\omega_L V_{\mathrm{peak}}} \tan(\theta) \quad (4.10)$$

here the supply current Ipeak, supply voltage Vpeak, line frequency ωL, and displacement θ are used to obtain the maximum capacitance. The amount of source impedance which is the 4-5% of the base impedance is considered. The required impedance is defined as Lreq.

$$L_f = L_{\mathrm{req}} + L_s \Rightarrow \frac{1}{4\pi^2 f_c^2 C_f} = L_{\mathrm{req}} + 0.04\left(\frac{1}{\omega_L}\right)\left(\frac{V_s^2}{P_o}\right) \quad (4.11)$$

A cutoff frequency is used which is in between the switching frequency fsw and the load frequency fL in the design.

$$f_L < f_c < f_{\mathrm{sw}}. \quad (4.12)$$

Usually fc is 1/10th of that of the fsw.

RESULTS and DISCUSSIONS

The simulation is developed using MATLAB Simulink as per the design and the control method thus discussed in the previous sections. The AC side supply followed by the BL buck boost converter is connected to the DC link capacitor and then it is followed by the three phase inverter which is controlled by the position sensor based control in fundamental frequency control.

The electromagnetic torque generated by the BLDC motor Te, speed in which motor is running N, and the current in the stator are analysed for the functioning of the proposed method. Inductor currents iLi1 iLi2 , the voltage across the switch Vsw1 ,Vsw2 and the current through the switch isw1 and isw2 for knowing whether the proposed converter is working desirably.

The simulation carried out is using both PI and ANFIS controller in converter's voltage output with difference in speed as the input. While both the PI and the ANFIS controller are used the ANFIS controller performed better in the speed settling time and DC voltage settling time control.

The overall Simulink diagram is split into two parts one is the control of DC converter's output voltage and the other is the hall sensor-based control of the BLDC motor. The DC output voltage control of the converter would provide the speed control of the BLDC motor while the hall sensor-based control just has a constant PWM from the inverter to move the BLDC motor.

Figure 4.4 (a) shows the Simulink diagram of the DC converter voltage control which is prime in speed control. Figure 4.4 (b) shows the hall sensor-based control of the BLDC motor.

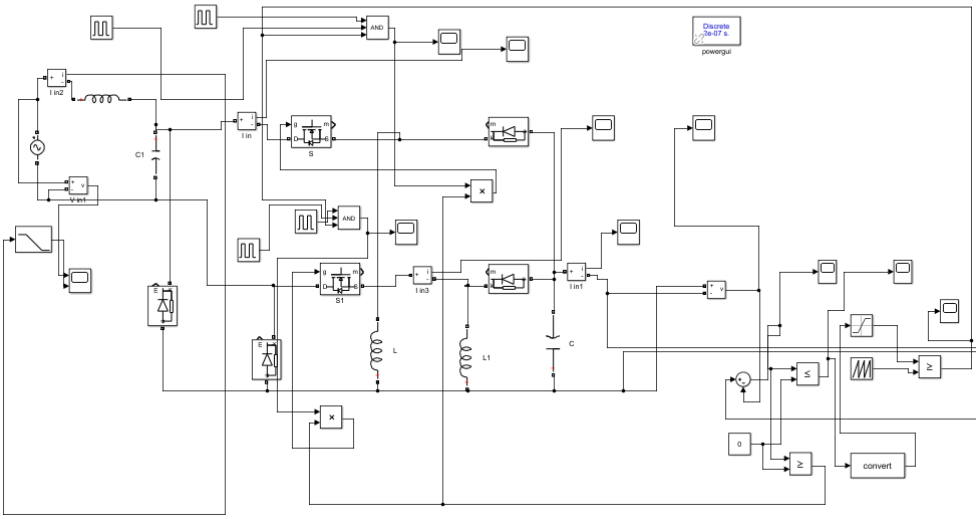

(a)

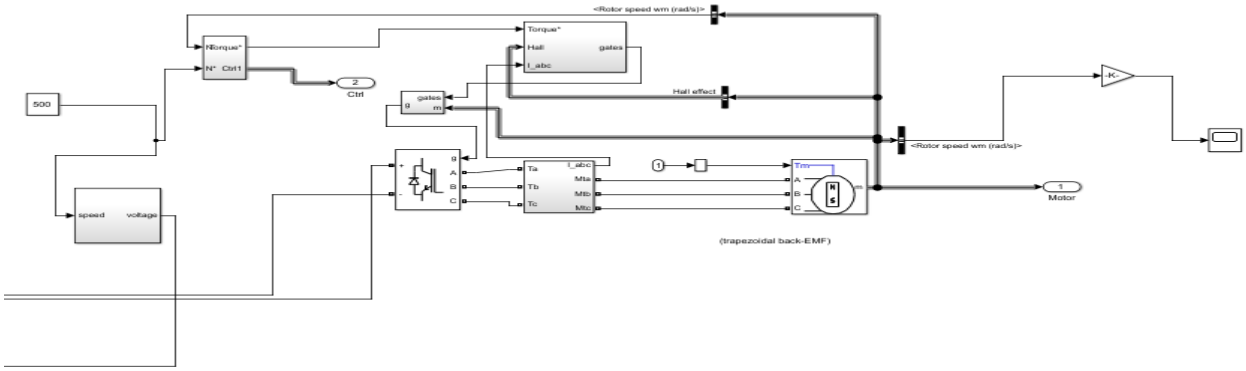

(b)

Figure 4.4 Simulink Diagram of the Overall Implementation (a) Speed control from DC voltage Control,(b) hall Sensor based position control

The parameters used for the PMBLDC motor and DC-DC converter construction is as shown in Table 4.1

Table 4.1 Motor and AC-DC converter parameters

SLno	Parameter	Value
1	Voltage	100V,5HP
2	Stator Phase resistance	0.2
3	Stator Phase inductance	8.5e-3
4	AC supply to the AC-DC converter	230V, 50Hz

5	LC filter AC input side	L=1.6e-3 Henry C=330e-9F
6.	Converter inductances	L=720e-6H L1=720e-6H
7.	Output capacitor	C=2200e-6
8.	AC-DC converter switching frequency	40Khz

The speed controller loop and the BLDC position control loop is discussed in the above sections of this chapter. The PI and the ANFIS controller are developed for the torque generation as the input to the hall sensor-based controller from the voltage to speed lookup table. The speed is estimated from the lookup table and is compared with the actual speed and the difference in speed is used to generate the torque reference which is provided to the controller which provides the speed control of the BLDC motor.

4.3.1 PI controller Outputs

The waveforms obtained from the PI controller-based implementation is as given in the following,

The AC-DC converter inductor current which would be working for one half cycle and the sinusoidal PWM controller in order to maintain the input voltage and current in phase. This is shown in Figure 4.5

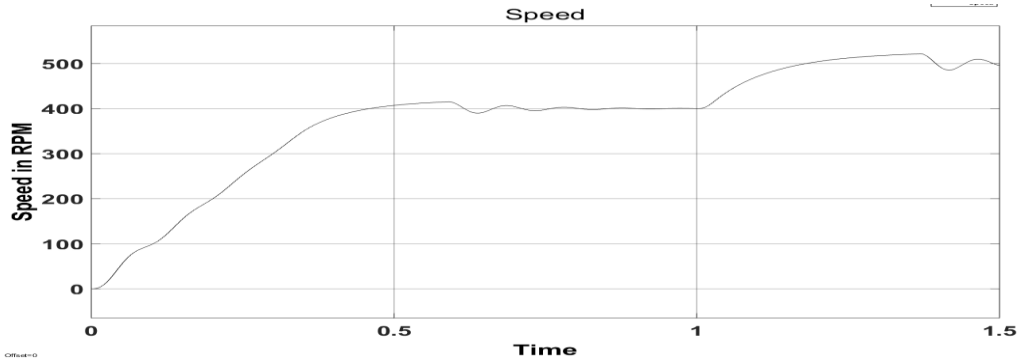

Figure Speed Response with different speed dynamic response

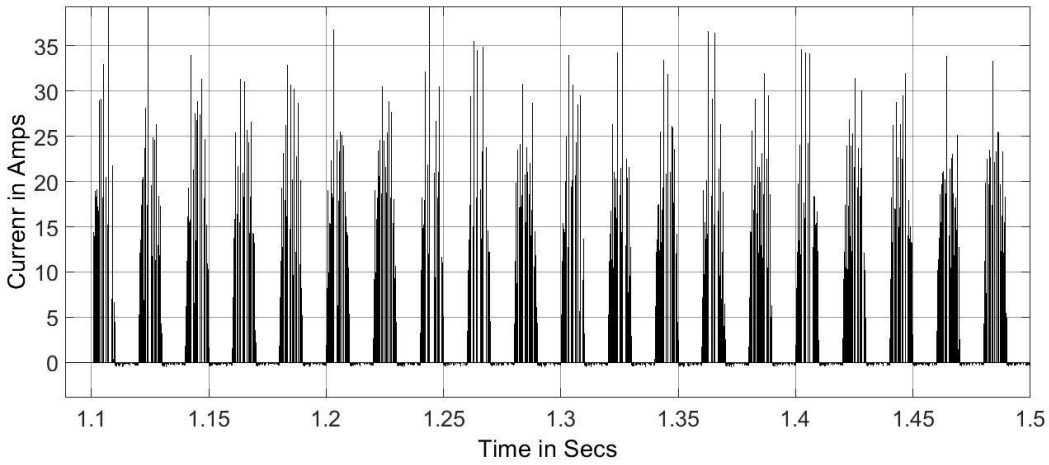

Figure 4.5 Inductor current in AC-DC converter

The output side inductor current in the AC-DC converter is as shown in Figure 4.6.

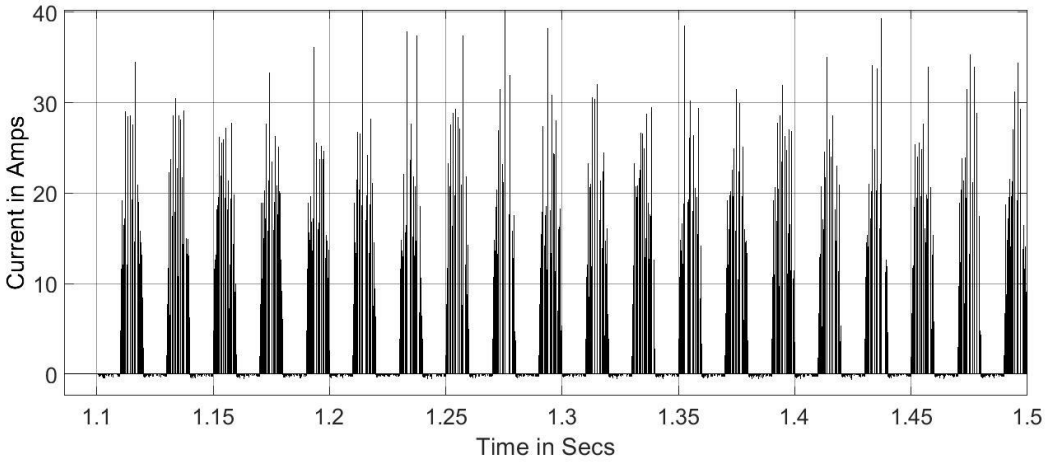

Figure 4.6 Inductor Current

The buck boost converter has higher current as the 230 V has to be converted to the range near 80V-100V. The output voltage of the AC-DC converter for a 500 RPM reference speed is as given in the following figure 4.7.

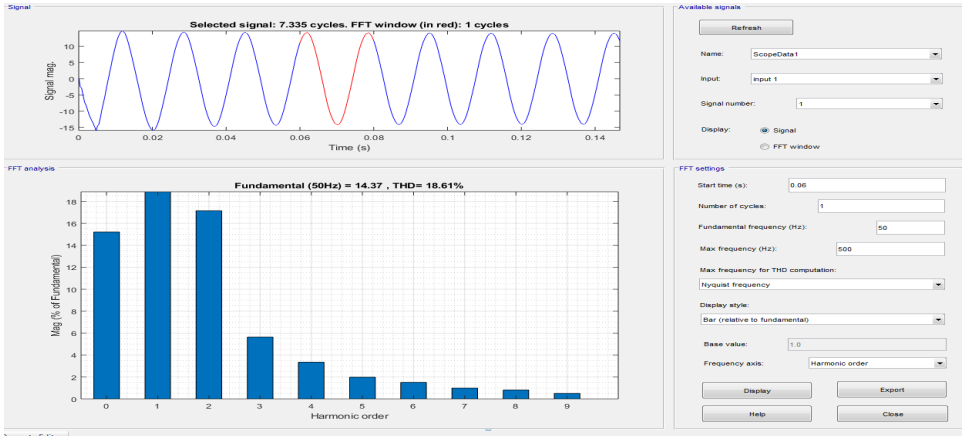

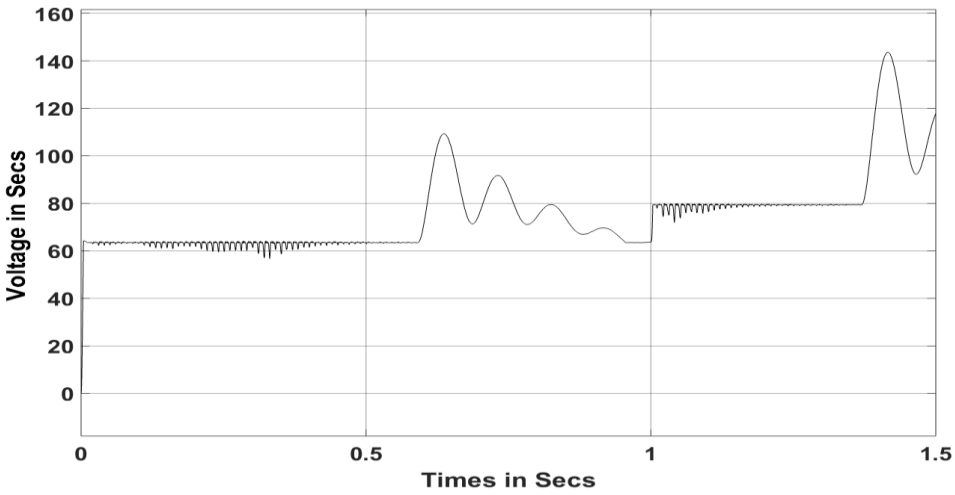

Figure 4.7 AC-DC converter voltage

The speed response for the 500 rpm reference speed is as shown in figure 4.8. It can be seen that the speed settles at 0.8 secs.

4.3.1 ANFIS IMPLEMENTATION

The neuro fuzzy implementation is carried out using the ANFIS toolbox in the Matlab Environment. The ANFIS command in the Matlab would use six arguments in total which include the option for training called trnOpt ,option of displaying dispOpt, data checking option chkData and the neural network training method and if the output has to be received all of them are optional. The training data that is got from the PI controller is used to train the ANFIS network. The error and the change in error that is given to the PI controller and the output of the PI controller is given as the complete data for training. While training the Fuzzy rules are developed in the ANFIS GUI. The error and change in error is defined as the input while the output of the PI controller is defined as the target vector. Usually, the ANFIS model uses the Takagi-Sugeno method that would create the fuzzy rules training environment for the fismat file.

4.3.2 ANFIS Model

The ANFIS model is similar to that of the FIS model except that it is also combined with the Neural Network model for training the FIS structure. The TS-FLC model is graphically represented as the ANFIS model. The ANFIS editor window would look like that which is in Figure 4.8.

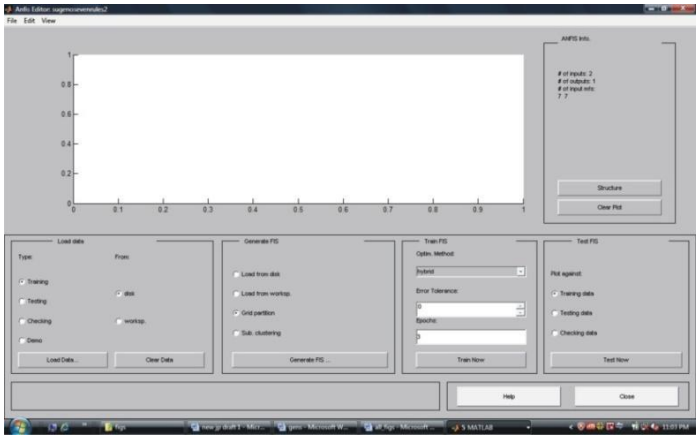

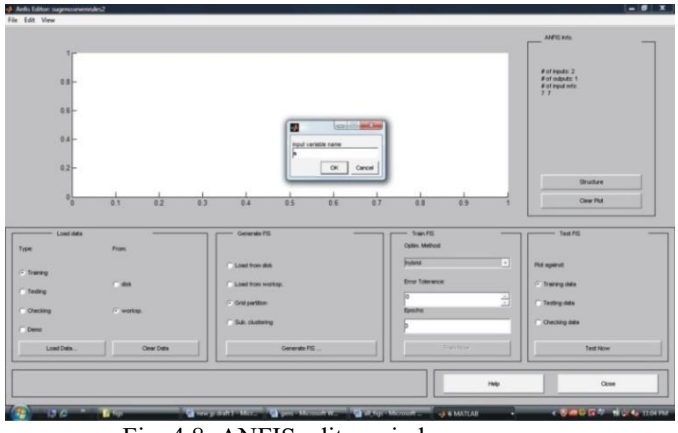

Fig. 4.8: ANFIS editor window

Fig. 4.9: ANFIS editor: Loading the data from the work space

Loading the training data which is stored as a .mat file in the same folder is used to get the input and the target data for training.

The structure of the NN trained can be as shown in the following figure as shown in the figure 4.10.

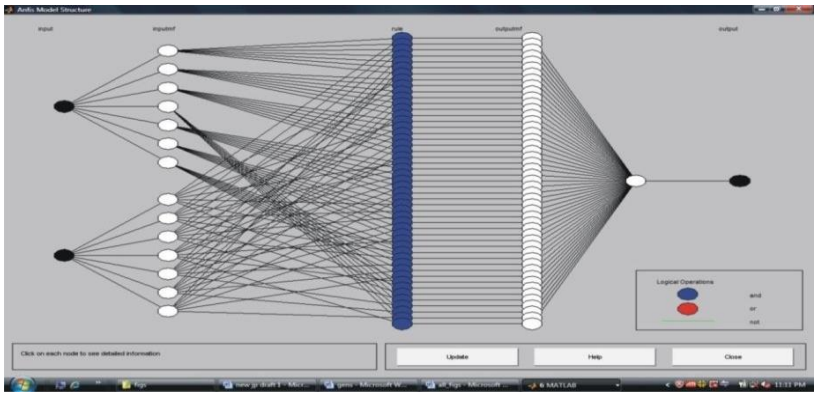

Fig.4.10 :ANFIS model with 2 inputs and 1 output showing the ANN architecture

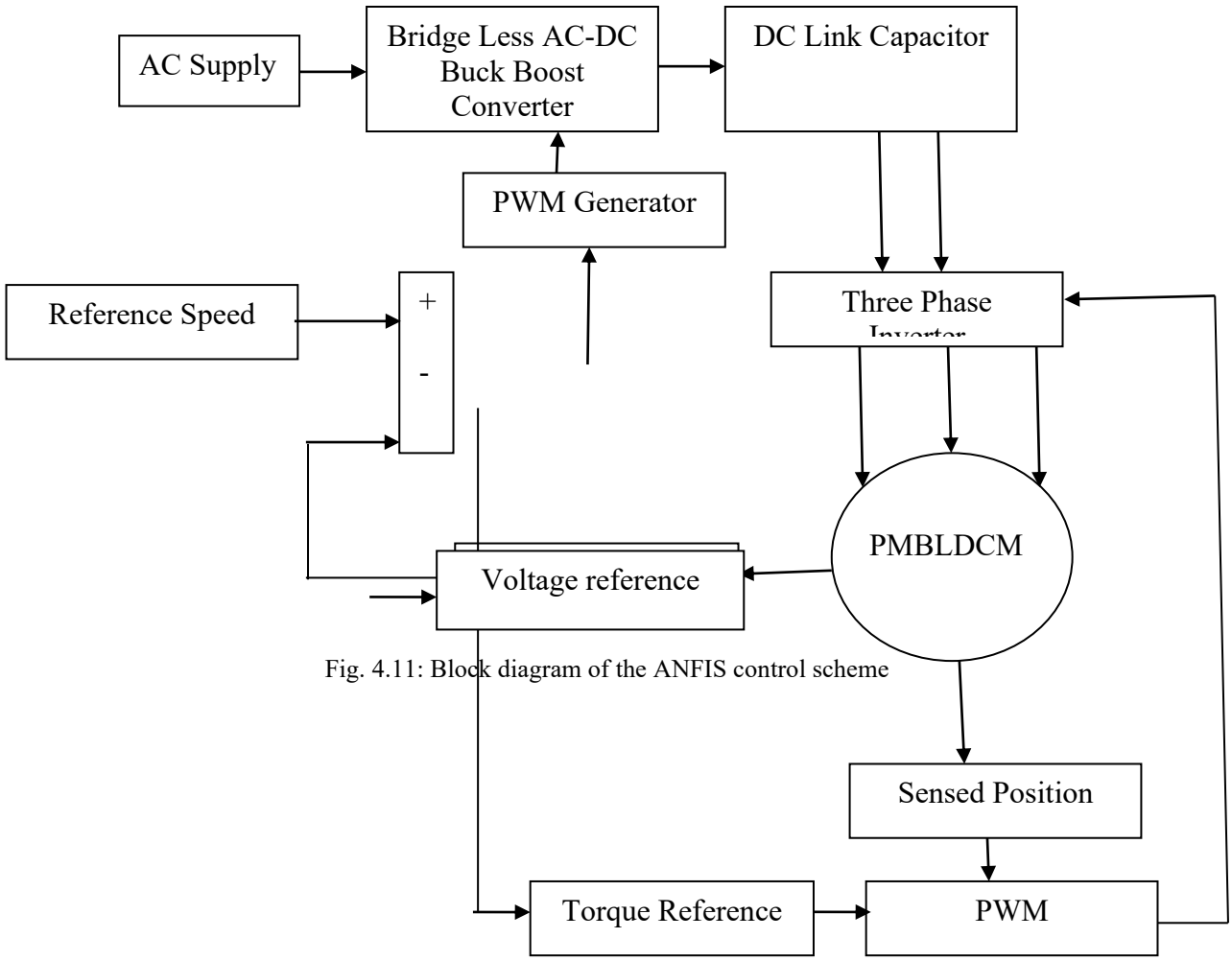

Fig. 4.11: Block diagram of the ANFIS control scheme

Block Diagram Explanation

The block diagram in the Figure 4.11 clearly mentions that the speed control of the BLDC motor is carried out using the ANFIS method used in the voltage control portion of the proposed converter. But the VSI is working with the PWM technique that is based on the hall sensor based positional control. The speed is controlled using the voltage control from the proposed converter by finding the difference of the speed and converting it to the reference voltage such that the speed is developed by applying the PWM which is needed to get the desired speed. There reference voltage is developed by the PI controller which gets the input from the speed sensor. The error and the change in error from the PI controller is utilized and the results output from the PI controller is utilized and the table involving the input and the target is given to the ANFIS controller.

$$e(k) = \omega ref - \omega r \quad (4.1)$$

$$\Delta e(k) = e(k) - e(k-1) \quad (4.2)$$

The error between the reference speed ωref and the actual speed ωr e(k) is the error and the difference between the error from the subsequent sample time is defined as Δe(k) .

Both the inputs error and change in error is fuzzified to get the input for the fuzzy logic implementation and 49 rules are getting generated to provide the learning on the fuzzy rules with NN layer in the ANFIS controller.

There are 7 such membership function for the ANFIS controller. Both the error and the change in error is introduced as the input for the fuzzy controller with the 7 membership functions defined as negative big(nb), negative medium(nm) negative small(ns) zero(ze), positive small(ps), positive medium(pm) and positive big(pb). The rules generated are as provided in the table 4.1

Table 4.1: Rule base for controlling the speed of PMBLDC using ANFIS

e□ *Δe*□	*Nb*	*nm*	*ns*	*ze*	*ps*	*pm*	*pb*
nb	*Nb*	*nb*	*nb*	*nb*	*nm*	*ns*	*ze*
nm	*Nb*	*nb*	*nm*	*nm*	*ns*	*ze*	*ps*
ns	*Nb*	*nm*	*ns*	*ns*	*ze*	*ps*	*pm*
ze	*Nb*	*nm*	*ns*	*ze*	*ps*	*pm*	*pb*
ps	*Nm*	*ns*	*ze*	*ps*	*ps*	*pm*	*pb*
pm	*Ns*	*ze*	*Ps*	*pm*	*pm*	*pb*	*pb*
pb	*Ze*	*ps*	*Pm*	*pb*	*pb*	*pb*	*pb*

After uploading these rules and training using the NN model the complete trained ANFIS model will be ready. Thus, model will further define the control of the PMBLDC for different loading and the speed reference conditions.

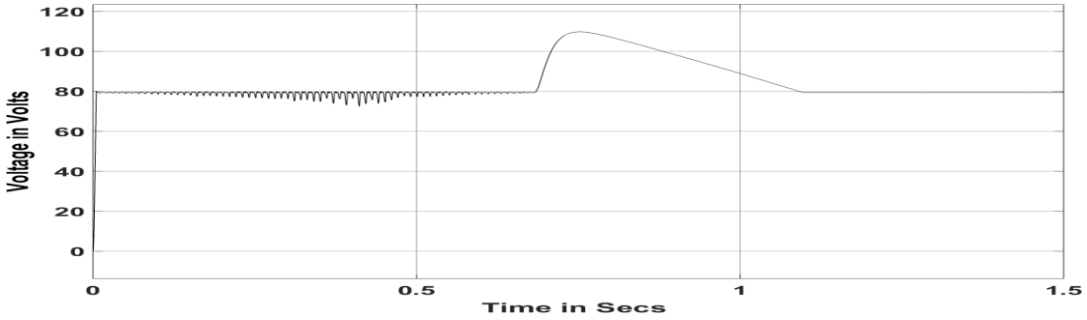

Figure DC-DC converter output Voltage

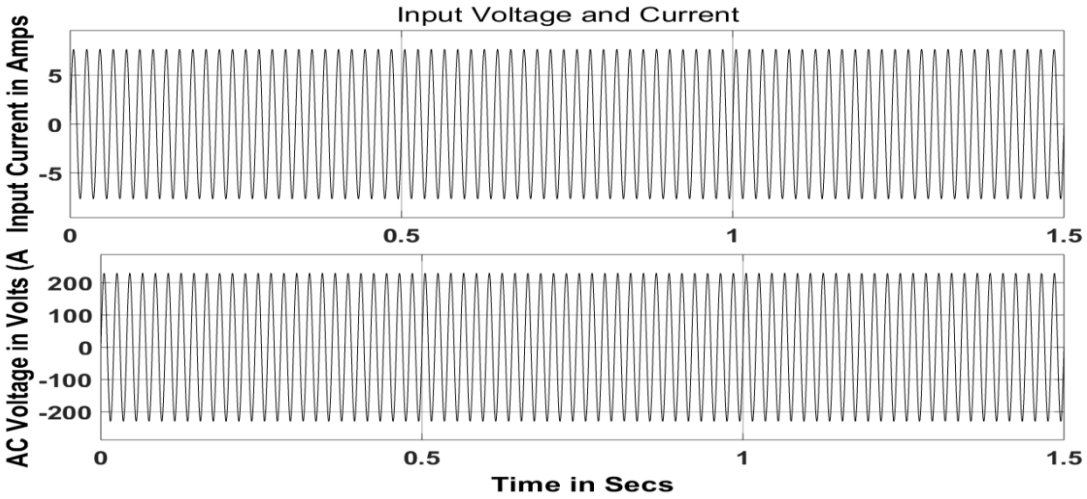

Figure AC Input Voltage and Current in Phase (UPF)

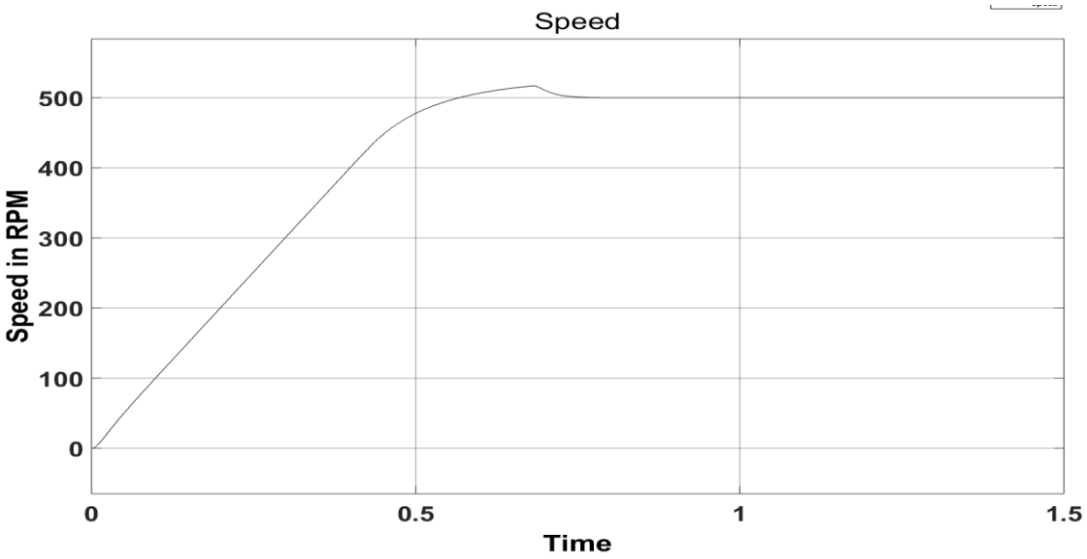

Figure Speed Control of ANFIS Controller with 500RPM reference

The AC-DC converter inductor current which would be working for one half cycle and the sinusoidal PWM controller in order to maintain the input voltage and current in phase. This is shown in Figure 4.

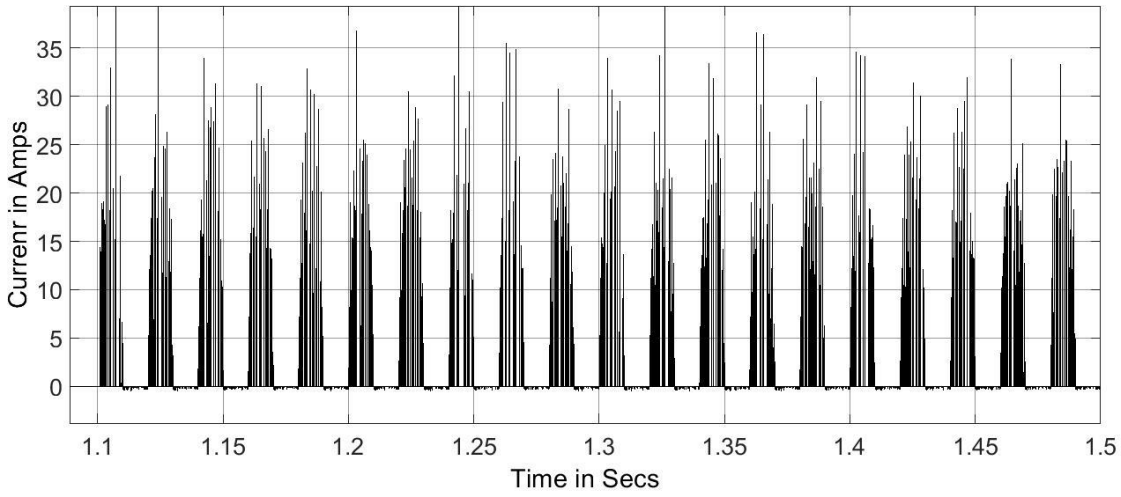

Figure 4. Inductor current in AC-DC converter

The output side inductor current in the AC-DC converter is as shown in Figure 4.6.

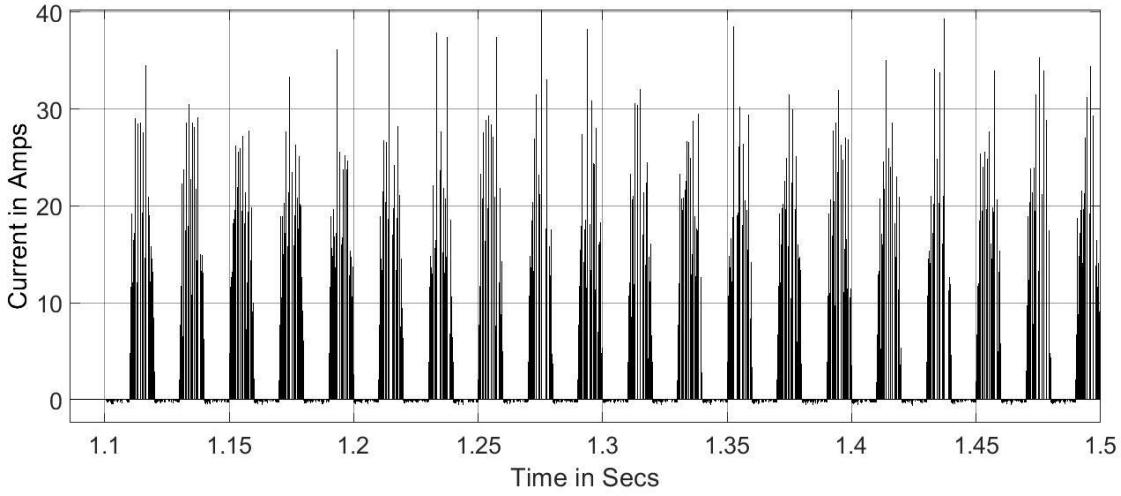

Figure 4.Inductor Current

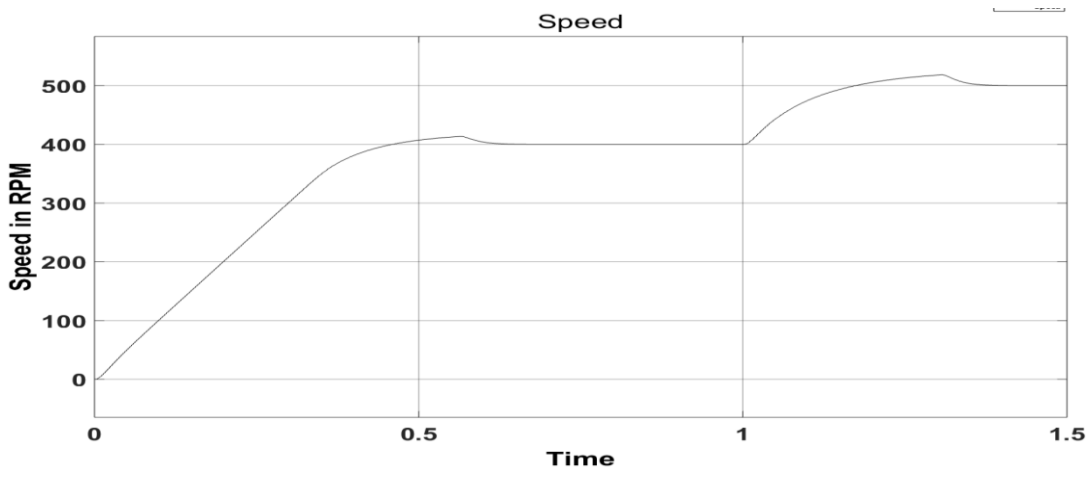

Figure ANFIS Speed Response with reference speed variation

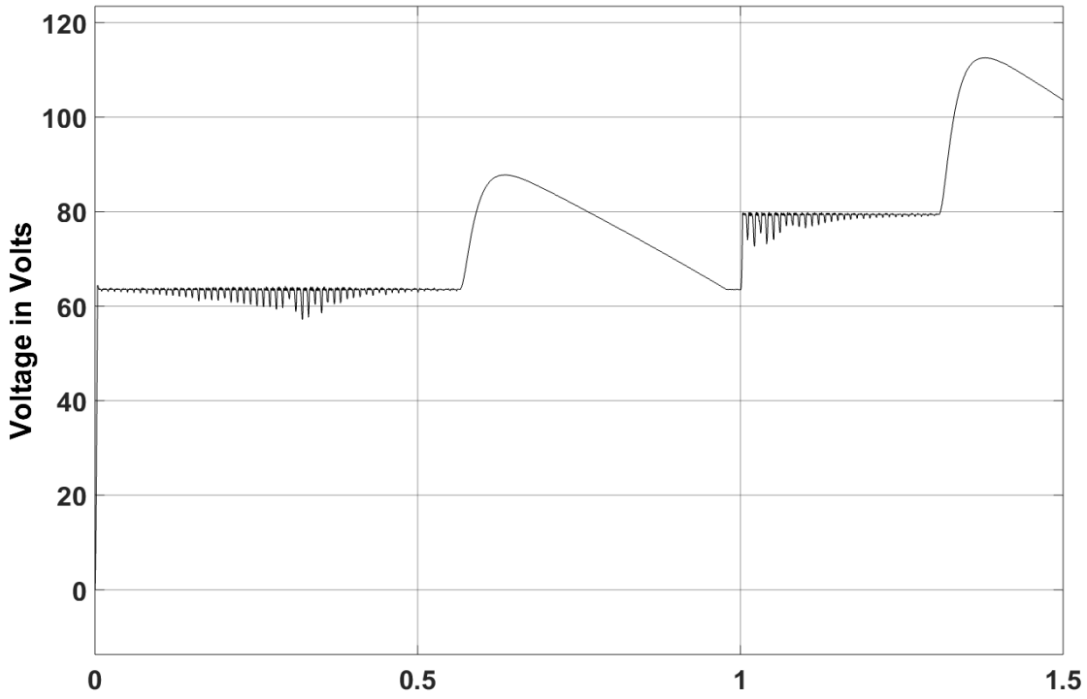

Figure Voltage response of the AC-DC Converter with variable speed reference

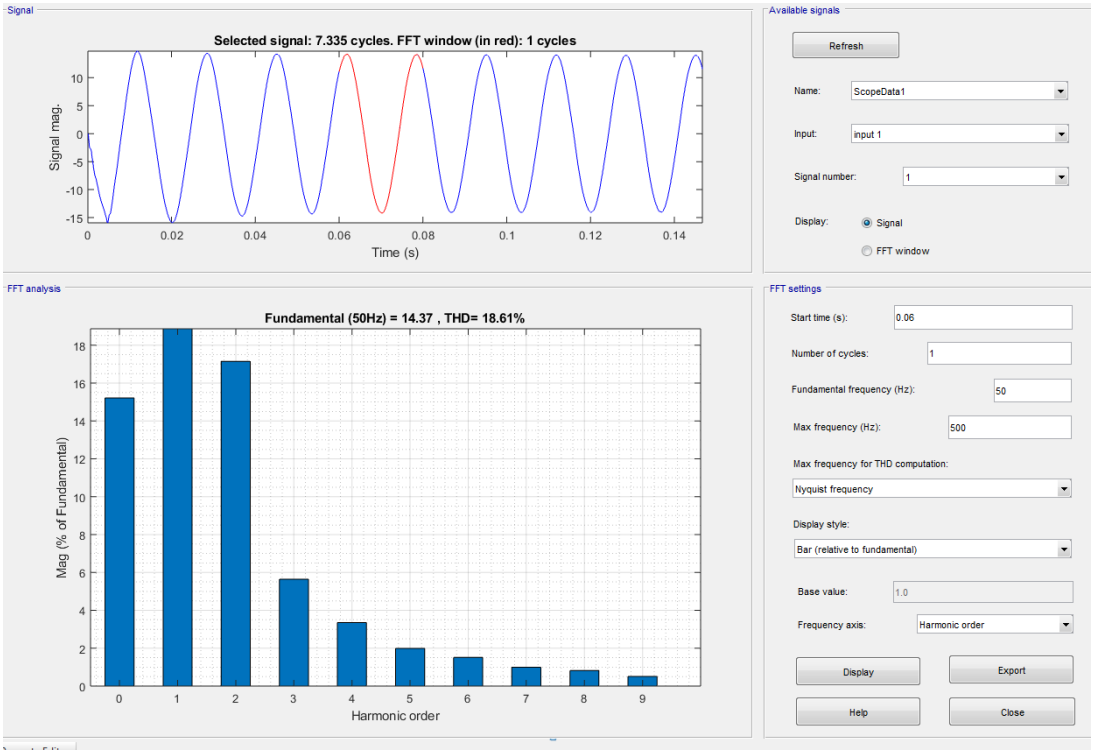

THD with ANFIS controller

The tabular column that tells the performance analysis of the PI controller and the ANFIS controller is as shown in Table 2.

Parameters	PI Controller Response	ANFIS Response
Settling time	1 sec	0.7 sec
THD	24%	16%
Peak overshoot	10%	15%
Rise time	.7secs	0.4secs
PF	.78	.84

The table infers that the overall performance of the ANFIS controller both in speed dynamics and the THD has performed better. Thus the suggestion that the ANFIS controller can be utilized.

CONCLUSION

Fundamental frequency controlled VSI based brushless buck boost converter is developed for a reduced switching loss-based implementation of the speed control of PMBLDC motor. The performance evaluation of the 100V 5HP motor was developed and validated for both the PI and the ANFIS controllers. The overall performance evaluation of the settling time and the THD is shown to be better from the Matlab based simulation carried out on the proposed converter-based speed control of PMBLDC motor. The removal of the bridge at the source side also has improved the PF at the source side to almost unity.

REFERENCES

1. Jeon, Y S, Mok, H S, Choe, G H, Kim, D K & Ryu, J S 2000, 'A new simulation model of BLDC motor with real back EMF waveform', Proc. of IEEE international conference, pp. 217-220.
2. Navidi, N, Bavafa, M & Hesami, S 2009, 'A new approach for designing of PID controller for a linear brushless DC motor with using ant colony search algorithm', IEEE power and energy engineering conference, pp. 1-5.
3. Balogh Tibor, Viliam Fedak & Frantisek Durovsky 2011, 'Modeling and simulation of the BLDC motor in MATLAB GUI', Proc. of IEEE international conference, pp.1403-1407.
4. Subhashish Bhattacharya, Leopoldo Resta, Deepak M Divan & Donald W Novotny 1999, 'Experimental comparison of motor bearing currents with PWM hard and soft-switched voltage-source inverters', IEEE Transactions on Power Electronics, vol. 14, no. 3, pp. 552-562.
5. Kyeong-Hwa Kim & Myung-Joong Youn 2002, 'Performance comparison of PWM inverter and variable DC link inverter schemes for high-speed sensorless control of BLDC motor', Electronics Letters, vol. 38, no. 21, pp. 1294-1295.
6. Wei Kun, Ren Junjun, Teng Fanghua & Zhang Zhongohao 2004, 'A novel PWM scheme to eliminate the diode freewheeling in the inactive phase in BLDC motor', Proc. of 35th Annual IEEE power electronics specialists conference, Aachen, Germany, pp. 2282-2286.
7. Dhawale, D D, Chaudhari, J G & Aware, M V 2010, 'Position control of four switch three phase BLDC motor using PWM control', Proc. of 3rd international conference on emerging trends in engineering and technology, pp. 374-378.

8. Alphonsa Roslin Paul & Mary George 2011, 'Brushless DC motor control using digital PWM techniques', Proc. of international conference on signal processing, communication, computing and networking technologies, pp. 733-738.

9. Krishna kumar, V & Jeevanandhan, S 2011, 'Four switch three phase inverter control of BLDC motor', IEEE 1st international conference on electrical energy systems, pp.139-144.

10. Voltage Source Inverter based control:

11. Tae-Sung Kim, Sung-Chan Ahn & Dong-Seok Hyun 2001, 'A new current control algorithm for torque ripple reduction of BLDC motors', Proc. of 27th annual conference of the IEEE industrial electronics society, pp. 1521-1526.

12. Byoung-Hee Kang, Choel-Ju Kim, Hyung-Su Mok & Gyu-Ha Choe 2001, 'Analysis of torque ripple in BLDC motor with commutation time', Proc. of IEEE international conference, Pusan, Korea, pp. 1044-1048. 185

13. Sang-Hyun Park, Tae-Sung Kim, Sung-Chan Ahn & Dong-Seok Hyun 2003, 'A simple current control algorithm for torque ripple reduction of brushless DC motor using four-switch three-phase inverter', Proc. of IEEE international conference, pp. 574-579.

14. Yong Liu, Zhu, Z Q & David Howe 2005, 'Direct torque control of brushless DC drives with reduced torque ripple', IEEE Transactions on Industry Applications, vol. 41, no. 2, pp. 599-608.

15. Ki-Yong Nam, Woo-Taik Lee, Choon-Man Lee & Jung-Pyo Hong 2006, 'Reducing torque ripple of brushless DC motor by varying input voltage', IEEE Transactions on Magnetics, vol. 42, no. 4, pp. 1307-1310.

16. Liu, Y, Zhu, Z Q & Howe, D 2006, 'Commutation torque ripple minimization in direct torque controlled PM brushless DC drives', Proc. of IEEE international conference, pp. 1642-1648.

17. Parag Upadhyay & Rajagopal, K R 2006, 'Torque ripple minimization of interior permanent magnet brushless DC motor using rotor pole shaping', Proc. of IEEE international conference.

18. Jianfei Yang, Yuwen Hu, Wenxin Huang, Jianbo Chu & Jin Gao 2009, 'Direct torque control of brushless DC motor without flux linkage observation', Proc. of IEEE international conference, IPEMC 2009, pp. 1934-1937.

19. Somesh Vinayak Tewari & Indu Rani, B 2009, 'Torque ripple minimization of BLDC motor with un-ideal back EMF', Proc. of 2nd international conference on emerging trends in engineering and technology, IEEE computer society, pp. 687-690

20. Chuang, H S, Yu-Lung Ke, & Chuang, Y C 2009, 'Analysis of commutation torque ripple using different PWM modes in BLDC motors', Proc. of IEEE international conference, pp. 1-6.

21. Salih Baris Ozturk, William C Alexander & Hamid A Toliyat 2010, 'Direct torque control of four-switch brushless DC motor with non-sinusoidal back EMF', IEEE Transactions on Power Electronics, vol. 25, no. 2, pp. 263-271.

22. Salih Baris Ozturk & Hamid A Toliyat 2011, 'Direct torque and indirect flux control of brushless DC motor', IEEE/ASME Transactions on Mechatronics, vol. 16, no. 2, pp. 351-360. 193

23. Sangsefidi, Y, Ziaeinejad, S & Shoulaie, A 2011, 'Torque ripple reduction of BLDC motors by modifying the non-commutating phase voltage', Proc. of international conference on electrical, control and computer engineering, Pahang, Malaysia, pp. 308-312.References should be given in alphabetical order. (font to be used: Verdana 8)

Table 1: Comparison of loads & Deflections

Analytical		Experimental	
Peak load (kN)	Midspan deflection (mm)	Peak load (kN)	Midspan deflection (mm)
87	44	76.9	43.3
102	37.1	106.9	48.2

Figure 1: Four-storey building model